Investigating *r*-Process Absorption Signatures in Stellar Spectra in Search of *r*-II Stars

Tino Wells†, Timothy Beers‡, Erika Holmbeck‡

†University of Hawai'i at Hilo ‡University of Notre Dame

Abstract

This research identified three possible first-pass constraints that isolate a significant percentage of tested *r*-II stars; (1) Using the absorption-line strengths of singly-ionized europium (Eu-II; 4129 Å), singly-ionized dysprosium (Dy-II; 4103 Å), and neutral iron (Fe-I; 4099 Å), we compute the ratios of each species with respect to iron, and define the constraint of 1.0 ≤ EW(Eu-II) / EW(Fe-I) ≤ 1.6 and 0.36 ≤ EW(Dy-II) / EW(Fe-I) ≤ 0.6, yielding six *r*-II stars in a sample of seven; (2) Using EW(Dy-II) as a function of metallicity, we identify a region that encompasses six out of seven *r*-II stars; (3) Utilizing a flavor of (2), we construct EW(Dy-II) as a function of effective temperature (T_{eff}), and define an additional region isolating all seven tested *r*-II stars. We suspect the collective implementation of these constraints will fitrate a given sample and quickly identify stars with similar characteristics and ultimately increase the discovery rate and overall number of this rare subclass.

Introduction

Astrophysical production of heavy elements via *r*-process—28% of all elements, and roughly 50% of those heavier than iron (see figure 2)—in the universe remains an open question. In order to investigate the nucleosynthesis of the r-process elements, we observe a specific category of stars formally known as metal-poor[1]. As defined in [1], the chemical abundance of observed stars (*) are compared to the sun (⊙) and given the following notation:

$$[A/B] \equiv \log_{10}(N_A / N_B)_* - \log_{10}(N_A / N_B)_\odot$$

… where N_A and N_B are the number of element A and element B atoms, respectively. Additionally, [1] defines a rare subclass of metal-poor stars, known as *r*-II or highly r-process-enhanced stars, that must meet two constraints regarding their chemical abundances: [Eu / Fe] > +1.0 and [Ba / Eu] < 0.0 (see table 1). That being noted, the full analysis of these stars, detection methods, and rate of discovery have various limitations, such as the time necessary in estimating the required parameters for stellar classification, and needing a relatively large telescope with a high-resolution spectrograph to observe them. In response to these issues, this research was focused on assessing different methods that isolate *r*-II stars to expedite the classification process. Furthermore, there have been previous attempts to do so, within this discipline by using the absorption-line strengths of singly-ionized europium, a known product of r-process enrichment, however, the results find it difficult to separate *r*-II stars from a similar subclass, known as *r*-I or moderately r-process-enhanced stars. This research carries out those efforts with singly-ionized dysprosium, another known product of r-process-enrichment, to address if dysprosium is a better metric in the isolation process (see figure 1).

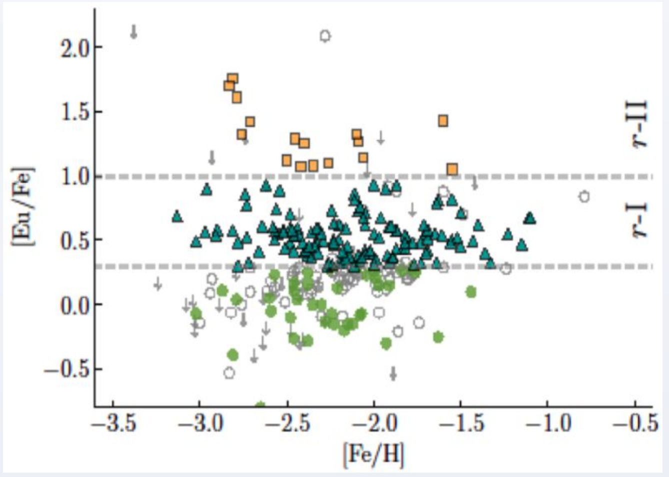

Figure 1: The figure to the left shows europium-iron abundance, [Eu / Fe], as a function of metallicity, or [Fe / H]. Here, notice the classification regime, with regards to [Eu / Fe] levels, on the vertical axis, represented by horizontal-dashed grey lines, where the top section corresponds with *r*-II stars, or the orange squares, the middle section corresponds with *r*-I stars, or the blue triangles, and the lower section relating to additional classifications. Also, notice how the separation factors between *r*-I and *r*-II stars only lies in the vertical direction, in which they are defined by. Because these two are not able to definitively diagnose/separate *r*-I and *r*-II stars using Eu alone, this research focuses on incorporating an additional element—a well known product of r-process-enrichment; dysprosium—to address whether or not dysprosium is a better metric for the isolation process. Figure courtesy of E. Holmbeck.

Methods

Defining constraints to classify possible *r*-II candidates falls into three flavors; first, we quantify the absorption-line strength of *r*-process elements by measuring two ionic species equivalent widths (EW; singly-ionized europium and dysprosium) and compute their ratio relative to the equivalent-width of neutral iron (see figure 3). Accurately measuring these equivalent widths is especially critical for dysprosium—EW(Dy-II)—due to being used in all three constraints. Furthermore, we use EW(Dy-II) as a function of [Fe / H] metallicity and define a region highly populated by *r*-II stars (see figure 4A). In figure 4B, notice the same EW(Dy-II) axis is used, however, now as a function of effective temperature (T_{EFF}) of the observed star. The python software that performs this filtration process takes a list of stars with corresponding measurements for EW(Eu-II), EW(Dy-II), EW(Fe-I), [Fe / H], and T_{EFF} and applies the constraints on the given sample, allowing the user to visually inspect which stars pass which constraints, and returns a list thereof for further analysis.

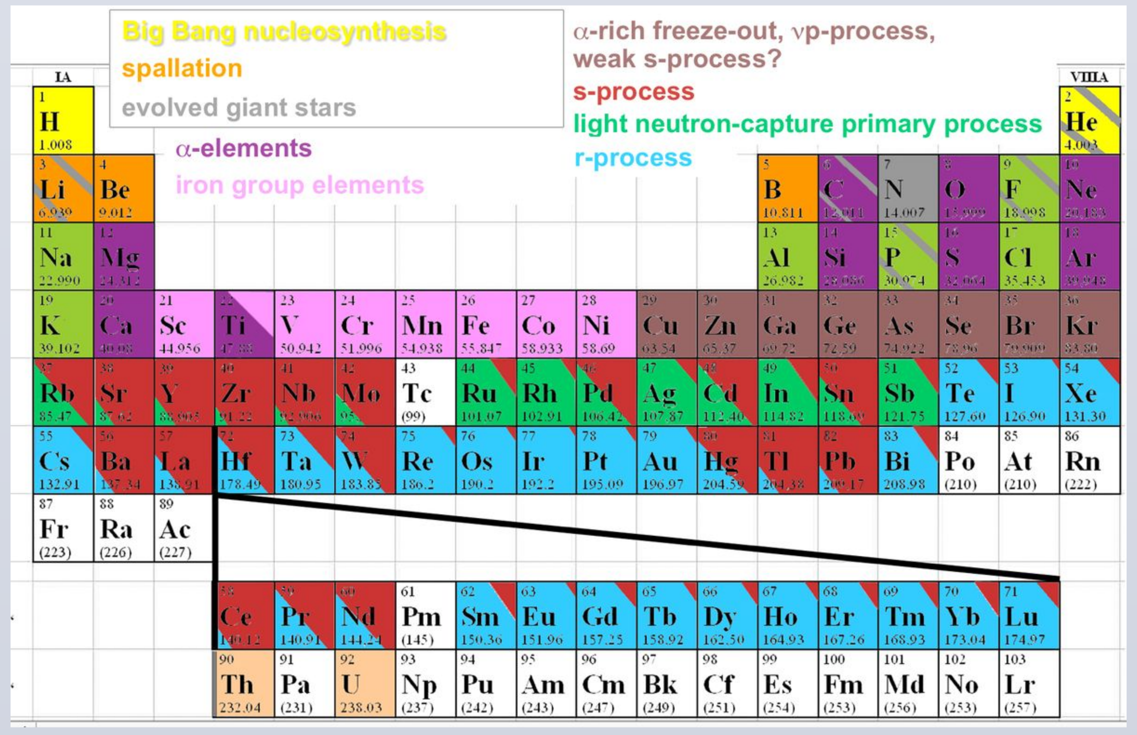

Figure 2: The above figure represents the common periodic table color coordinating each element with their corresponding nucleosynthetic origins. Notice atomic numbers 52-83 being produced via r-process, composing roughly 30% of all known elements, and roughly 50% of those heavier than iron. Courtesy A. Frebel.

Results

After measuring the absorption-line strengths of the three species, the primary constraints constructed isolate *r*-II stars as follows: 1.0 ≤ EW(Eu-II) / EW(Fe-I) ≤ 1.6 and 0.36 ≤ EW(Dy-II) / EW(Fe-I) ≤ 0.6 (see figure 3). This region is composed of 11 stars in total, six of which are *r*-II stars, three are *r*-I stars, and two of unknown classification(s). Following these constraints, figure 4A (top-panel) shows the cut-off region of [Fe / H] metallicity as a function of EW(Dy-II), where stars rightward of the dashed line have been isolated for consideration. This region consists of 16 stars in total, and of these stars, we see six *r*-II stars, four *r*-I stars, and six of unknown classification(s). Lastly, in figure 4B (bottom-panel), displays the cut-off region with EW(Dy-II) as a function of T_{EFF} where we now isolate all sevel tested *r*-II stars, with 13 *r*-I stars, and four stars of unknown classification(s), rightward of the dashed line. The collective implementation of these constraints, on a sample of 107 stars in total, produced a list of nine stars in total, six of which are *r*-II stars, and three *r*-I stars, converging to a 66% success rate of all tested stars, and 85% success rate of *r*-II stars individually.

[Fe / H]	Term	Acronym
> +0.5	Super metal-rich	SMR
~ 0.0	Solar	—
< -1.0	Metal-poor	MP
< -2.0	Very metal-poor*	VMP
	…	
Neutron-capture-rich Stellar Classifications		
r-I*	0.3 < [Eu / Fe] < +1.0	[Ba / Eu] < 0
r-II*	[Eu / Fe] > +1.0	[Ba / Eu] < 0
s	[Ba / Fe] > +1.0	[Ba / Eu] > +0.5
r/s	0.0 < [Ba / Eu] < +0.5	—

Table 1: Stellar classification summary as outlined in [1]. This research focused on the stellar classification of very metal-poor (VMP) stars, with primary attention on the subclass of *r*-II stars. All categories used in this research are indicated via (*).

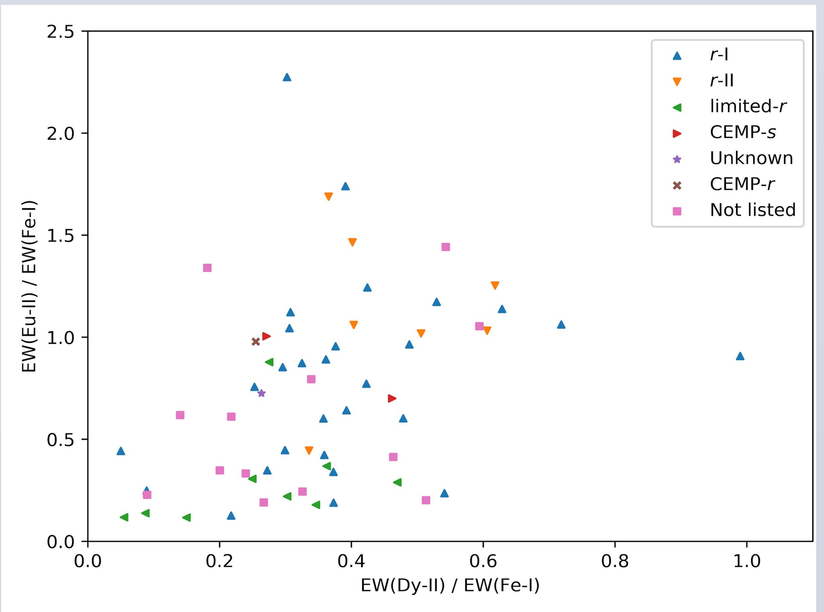

Figure 3: The figure to the right shows a sample of stars from a number of stellar subclassifications. Notice how the *r*-II stars, labeled as upside-down orange triangles, seem to cluster together in the middle of the frame. By constructing the limits of 1.0 ≤ EW(Eu-II) / EW(Fe-I) ≤ 1.6 and 0.36 ≤ EW(Dy-II) / EW(Fe-I) ≤ 0.6, we restrict a region in the equivalent-width that isolates a total of 11 stars, where six out the the seven testing *r*-II stars are located within this region.

Discussion

The three constraints identified from this research enables a relatively decent first-pass isolation process, however, the entirety of the analysis process requires much more time. As this research was devoted to constructing a method to identify possible *r*-II candidates—essentially prioritizing stars with similar characteristics—we have discussed additional methods that can perform much better. Specifically, using a form of neural network that will predict the stellar parameters explicitly focused on those necessary in defining *r*-II stars is currently under development. Although this may take some additional time, the neural network is believed to produce much more accurate and usable information, including an estimation for overall [Fe / H] metallicity, and with a growing population of known *r*-II stars, become more and more accurate over time.

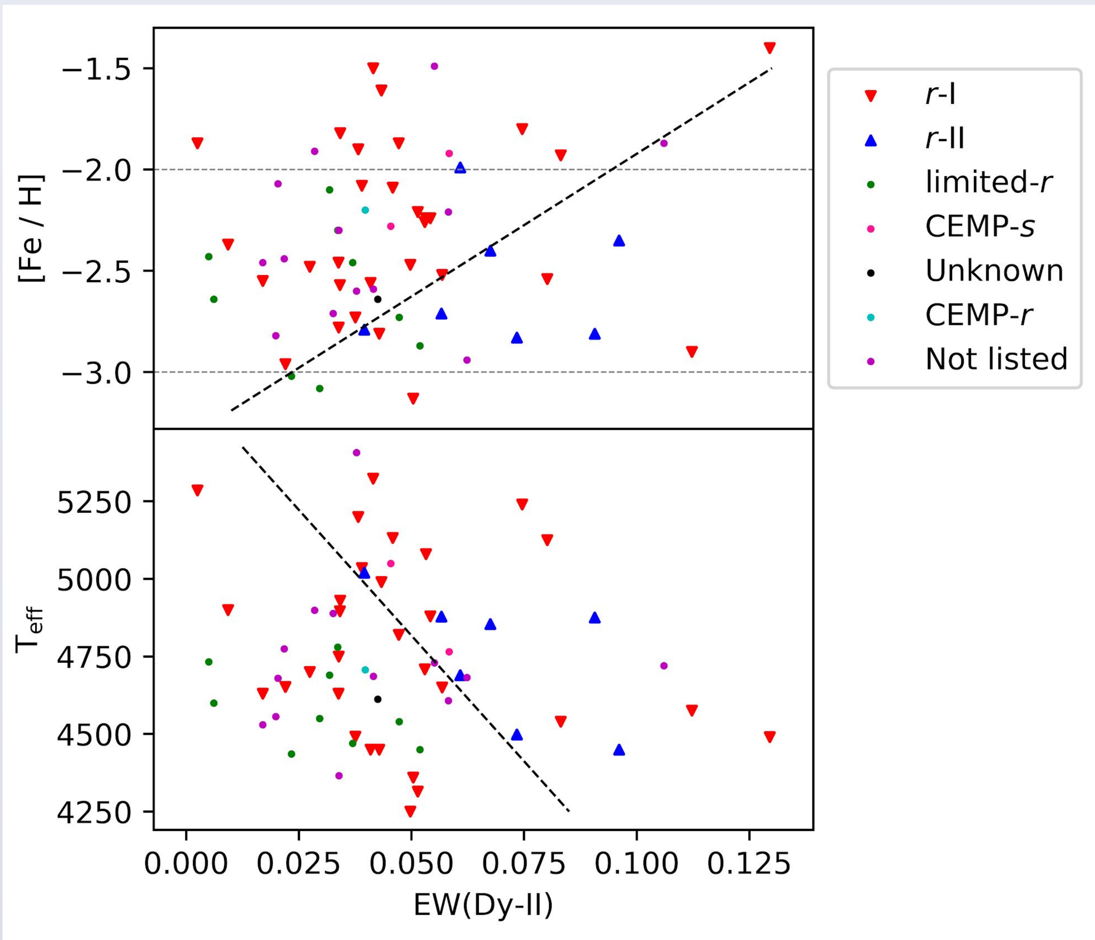

Figure 4: The figure above contains two constraints for the filtration process, where the top panel shows metallicity as a function of EW(Dy-II) and T_{eff} as a function of EW(Dy-II) in the bottom-panel. For both panels, stars rightward of the blacked dashed-line pass the filtration constraints and will be considered higher-priority stars for subsequent analysis.

Acknowledgements

I would first like to thank the National Science Foundation, the Research Experience for Undergraduates program (REU), and the REU coordinator at the University of Notre Dame, Dr. Umesh Garg, for funding and allowing my opportunity to conduct this research. I would also like to thank University of Notre Dame graduate student, Erika Holmbeck, for her explicit help, guidances, and expertise on this project, and a special thank you to my advisor, Dr. Timothy Beers for his expertise and allowing REU student(s) to aid his research team.

References

[1] Beers, T., & Christlieb, N. 2005, *Annu. Rev. Astron. Astrophys.* 43:531-580.